Journal of Solid State Chemistry 182 (2009) 2972–2976

Contents lists available at ScienceDirect

Journal of Solid State Chemistry

journal homepage: www.elsevier.com/locate/jssc

TiO_2 nanoparticles incorporated with $CuInS_2$ clusters: preparation and photocatalytic activity for degradation of 4-nitrophenol

Shi-Zhao Kang [a,*], Yi-Kai Yang [b], Wenbo Bu [c], Jin Mu [b]

[a] Department of Chemical Engineering, Shanghai Institute of Technology, 120 Caobao Road, Shanghai 200235, China
[b] Department of Chemistry, East China University of Science and Technology, P.O. Box 427, 130 Meilong Road, Shanghai 200237, China
[c] State Key Lab of High Performance Ceramics and Superfine Microstructures, Shanghai Institute of Ceramics, Chinese Academy of Sciences, 1295 Ding-xi Road, Shanghai 200050, China

ARTICLE INFO

Article history:
Received 25 June 2009
Received in revised form
9 August 2009
Accepted 11 August 2009
Available online 15 August 2009

Keywords:
TiO_2
$CuInS_2$
Nanoparticles
Photocatalytic activity
4-Nitrophenol

ABSTRACT

TiO_2 nanoparticles incorporated with $CuInS_2$ clusters were prepared in a solvothermal process and characterized with X-ray diffraction (XRD), transmission electron microscopy (TEM), and energy-dispersion X-ray analysis (EDX). Compared with pure TiO_2 nanoparticles, the TiO_2 nanoparticles incorporated with $CuInS_2$ clusters display higher photocatalytic activity with 99.9% of degradation ratio of 4-nitrophenol after 2 h irradiation. In order to investigate the effect of the $CuInS_2$ clusters on the photocatalytic activity of TiO_2 nanoparticles, diffuse reflectance UV–Vis spectra (DRS), photoluminescence (PL) spectra, and photocurrent action spectra were measured. The results indicate that the enhanced photocatalytic activity is probably due to the interface between TiO_2 and $CuInS_2$ as a trap of the photogenerated electrons to decrease the recombination of electrons and holes.

© 2009 Elsevier Inc. All rights reserved.

1. Introduction

With rapid development of industry, the pollution from chemicals becomes a serious problem. Among various pollutants, nitrophenols are some of the most refractory substances due to their high stability and solubility in water. The purification of wastewater contaminated by nitrophenols is very difficult because they are resistant to the traditional treatment [1]. Fortunately, it was found that nitrophenols would undergo photolysis under irradiation, suggesting that the photolysis of nitrophenols seems a promising treatment route. However, the photolysis efficiency of nitrophenols is generally very low if the photocatalyst is absent [2]. Therefore, the highly efficient photocatalysts are a key in the photolysis of nitrophenols.

$CuInS_2$ (CIS) is thought to be the most promising material for photovoltatic applications, owing to its high absorption coefficient and direct band gap of 1.55 eV which is well matched to the solar spectrum [3]. In order to prepare a highly efficient solar cell, CIS as a p-type semiconductor has been widely compounded with n-type TiO_2 via layer by layer deposition. And these solar cells can exhibit high photoefficiency [4,5]. The theoretical analysis and experimental results show that the high photoefficiency of the solar cells based on TiO_2 and CIS is ascribed to the p–n junction between TiO_2 layers and CIS layers which leads to decrease of the recombination of electrons and holes. Following this idea, it can be expected that the TiO_2/CIS composite ought to possess high photocatalytic activity when it is used in the photolysis of nitrophenols as a photocatalyst. However, to our best knowledge, there are few reports on the photocatalytic activity of the TiO_2/CIS composite. One possible reason is that the layer by layer film of the TiO_2/CIS composite is unsuitable as a photocatalyst due to its relatively smaller surface and interface between TiO_2 and CIS. The shortcoming can be overcome if some CIS clusters are incorporated into TiO_2. Moreover, CIS can be produced on a large scale at less cost, which is encouraging for the potential application. Therefore, TiO_2 incorporated with the CIS clusters can be expected to be an excellent photocatalyst with high efficiency and low cost. Unfortunately, it is unclear so far if the TiO_2 nanoparticles incorporated with the CIS clusters can exhibit high photocatalytic activity.

Now, a great deal of attention is paid to the photocatalytic degradation of nitrophenols in the aqueous dispersions containing TiO_2 [1,6,7]. However, the efficiency is still no satisfactory enough for the TiO_2-based photocatalysts. The investigation showed that modification of the TiO_2 surface with noble metals, such as Ag, Pd, Au, and Pt, etc., is one of the most successful ways to improve the TiO_2 photoefficiency [8]. However, high cost limited the large scale application of TiO_2 modified with noble metals. Recently, the p–n junction was introduced in the TiO_2-based photocatalysts in order to enhance the TiO_2 photoefficiency. For example, Ye et al.

* Corresponding author. Fax: +86 21 64252485.
E-mail address: kangsz@sit.edu.cn (S.-Z. Kang).

0022-4596/$ - see front matter © 2009 Elsevier Inc. All rights reserved.
doi:10.1016/j.jssc.2009.08.014

found that the photocatalytic activity of TiO_2–Fe_3O_4 was remarkably improved compared with that of pure TiO_2 [9]. The investigation showed that this phenomenon was attributed to the p–n junction between n-type TiO_2 and p-type $FeTiO_3$ formed in the preparation process. Thus, it can be deduced that introduction of the p–n junction in the TiO_2-based photocatalysts may be a possible alternative to enhance the photocatalytic activity of TiO_2 for the photolysis of nitrophenols.

In this work, the TiO_2 nanoparticles incorporated with the CIS clusters were synthesized successfully via a solvothermal process. The high photocatalytic activity of the TiO_2 nanoparticles incorporated with the CIS clusters was investigated by examining photocatalytic degradation of 4-nitrophenol at room temperature. Furthermore, the role of the CIS clusters in the TiO_2-based photocatalyst is discussed by using UV–Vis spectra, photoluminescence spectra, and photocurrent action spectra.

2. Experimental

2.1. Preparation of the photocatalyst

The reagents were obtained from commercial sources and used as received. In a typical procedure, $Ti(OC_4H_9)_4$ (15 mL) and acetic acid (4 mL) were added into 60 mL ethanol under vigorous stirring. The mixture was heated to 50 °C and kept stirring for 30 min. Then, a mixture (pH = 3) of ethanol (20 mL) and water (1 mL,) was added droplet to the solution of $Ti(OC_4H_9)_4$. After stirred for 2 h, the sol of TiO_2 was obtained.

The $CuInS_2$ precursor was prepared according to the procedure reported previously [10]. At first, indium chloride (2 mmol) was added into the ethanol (30 mL) containing copper chloride (2 mmol). After stirred for a few minutes, thiourea (3.5 mmol) was mixed with the above solution. Then, the mixture was stirred for 10 min. Finally, the $CuInS_2$ precursor was prepared.

TiO_2 sol (30 mL) was mixed with various volume of the $CuInS_2$ precursor suspension according to the contents of $CuInS_2$ in the samples. After stirred vigorously for 30 min, the mixture was transferred into a 50 mL Teflon-lined stainless-steel autoclave and underwent solvothermal treatment at 180 °C for 16 h. Subsequently, it was cooled down to room temperature. The gel obtained was collected by centrifugation and washed several times with distilled water and ethanol, respectively. Finally, the precipitate was dried in vacuum at 80 °C for 5 h. The samples were noted as **T1** (TiO_2 incorporated with 0.5 at% $CuInS_2$) and **T2** (TiO_2 incorporated with 5 at% $CuInS_2$), respectively.

2.2. Photocatalytic degradation of 4-nitrophenol

The homemade "solar box" equipped with a 300 W high-pressure Hg lamp ($\lambda = 365$ nm) was used for the photocatalytic degradation of 4-nitrophenol. In order to remove the infrared light, the lamp was equipped with a water jacket. The photocatalytic experiments were carried out in a reactor containing 25 mL aqueous 4-nitrophenol (20 mg L^{-1}) and the catalyst (25 mg). The pH value of the system was adjusted to 4 in order to eliminate the self-sensitized photolysis of 4-nitrophenol [11]. The experiments were performed in open air with magnetically stirring to supply enough oxygen for the photodegradation. The distance between the lamp and the reactor is 20 cm. After a given irradiation time, the concentration of 4-nitrophenol was monitored by measuring its absorbance at 317 nm. The degradation efficiency was calculated according to the equation:

$$\text{Degradation}\ (\%) = \frac{A_0 - A}{A_0} \times 100\% \quad (1)$$

where A_0 represents the initial absorbance of 4-nitrophenol, A the absorbance after irradiation.

2.3. Fabrication of cells and the optoelectronic measurement

The TiO_2 nanoparticles incorporated with $CuInS_2$ clusters were dispersed in the distilled water. Then, the films of the TiO_2 nanoparticles incorporated with $CuInS_2$ clusters were prepared on the ITO glass substrates by using the doctor blade technique. After the films were dried under ambient conditions, they were used to fabricate the cells according to the procedure reported by Smestad et al. [12]. HY-914 resin was used to encapsulate circuit.

A 500 W Xe lamp with a monochromator was used as the light source. The light intensity was about 750 W m^{-2}. The illumination area on the electrode was about 1.5 cm^2. The generated photocurrent signal was collected by using a lock-in amplifier (Stanford instrument SR830 DSP, USA) synchronized with a light chopper (Stanford instrument SR540). The current–voltage (I–V) curves were recorded with a Keithley 2400 sourcemeter (Keithley Instruments, Inc., USA).

2.4. Characterization

The powder XRD analysis was measured on a Rigaku 2550D/max VB/PC X-ray diffractometer (Japan) using Cu$K\alpha$ radiation ($\lambda = 0.154056$ nm). The morphology of the sample was characterized on a FEI Technai 20 high-resolution transmission electron microscope (FEI Co., Netherlands). The EDX pattern was taken with a JEOL JSM-6360LV electron microscopy (Japan). The UV–Vis spectra of the aqueous 4-nitrophenol were recorded with a UV-2102 PCS spectrophotometer (Unico Co., China). The UV–Vis spectra of the solid samples were measured on a Shimadzu UV-3101PC UV–Vis-NIR scanning spectrophotometer (Japan). The PL spectra of the samples were obtained using a Varian Cary Eclipse fluorescence spectrophotometer (USA). The excitation wavelength was 325 nm.

3. Results and discussion

The XRD patterns of the pure TiO_2 nanoparticles, **T1**, and **T2** are shown in Fig. 1. For the pure TiO_2, **T1**, and **T2**, the sizes of the particles calculated from Scherrer formula [13], are all approximately 9 nm. Meanwhile, it can be observed that there

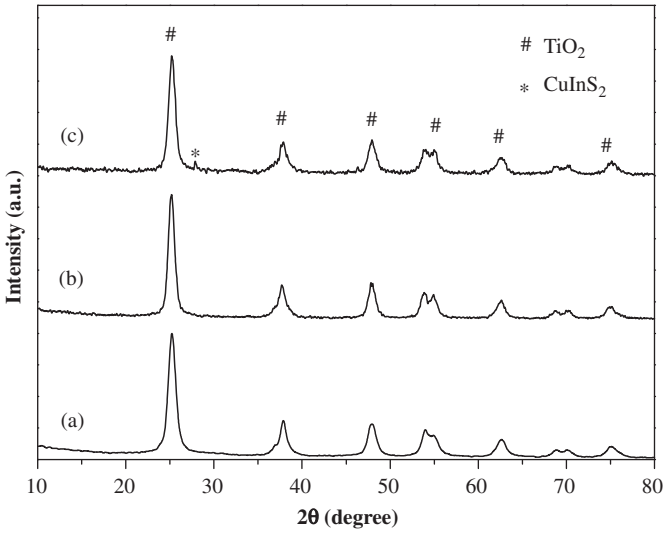

Fig. 1. XRD patterns of the pure TiO_2 nanoparticles (a), **T1** (b), and **T2** (c).

exist four peaks at 25.2°, 37.9°, 48.0°, and 62.5° in all of XRD patterns, corresponding to the (101), (004), (200), and (204) planes of anatase TiO_2 (Powder Diffraction File no. 21-1272), respectively. This result displays that the obtained TiO_2 particles are nanoscale and possess the anatase phase. Moreover, these diffraction peaks do not shift with introduction of Cu, In, and S element, implying that Cu, In, and S elements are segregated in the form of small $CuInS_2$ clusters. The experimental result below also confirms this assumption. When the content of $CuInS_2$ clusters increases to 5 at%, a weak peak at 27.9°, which is attributed to the (112) plane of the tetragonal $CuInS_2$ (Powder Diffraction File no. 27-159), appears (curve c). Although the diffraction peak of $CuInS_2$ is not observed in the XRD pattern of **T1**, it cannot be presumed from the above phenomenon that Cu, In, and S elements are embedded within the TiO_2 matrix forming a solid solution. One possible explanation is that the $CuInS_2$ clusters are too small to give well-defined diffraction peaks [14]. These results imply that the $CuInS_2$ clusters are incorporated in TiO_2 nanoparticles.

In order to substantiate the formation of TiO_2 nanoparticles incorporated with the $CuInS_2$ clusters, we measured the morphology of **T1** using TEM, as shown in Fig. 2a. The nanoparticles with the mean diameter of approximately 10 nm are clearly observed, which is close to the one deduced from XRD measurement and exhibit a relatively narrow size distribution (Fig. 2b). Moreover, further evidence for the composition of **T1** was obtained by EDX analysis (not shown here). The results show that the distribution of the elements is homogeneous in **T1. T1** is composed of the elements Ti, Cu, In, and S. The Cu/In/S ratio is very close to the stoichiometric composition of $CuInS_2$ (Cu/In/S = 1:1:2) within experimental error. Therefore, in combination with the results of XRD, the component of the as-synthesized sample can be defined as TiO_2 and $CuInS_2$. The $CuInS_2$ clusters are incorporated in TiO_2 nanoparticles.

Fig. 3 shows the diffuse reflectance UV–Vis spectra of the pure TiO_2 nanoparticles, **T1**, and **T2**. As can be seen from Fig. 3, there exists a broad intense absorption band below 400 nm for three samples, which should be ascribed to a charge-transfer process from the valence band to the conduct band [15]. According to the formula reported by Ghosh et al. [16], the energy gap (Eg) values for all the samples are estimated to be approximately 3.28 eV (the pure TiO_2 nanoparticles), 3.28 eV (**T1**), and 3.27 eV (**T2**), respectively. These results show that introduction of Cu, In, and S elements does not influence the charge-transfer process of TiO_2 nanoparticles, suggesting that the Cu, In, and S elements are segregated in the form of small $CuInS_2$ clusters rather than embedded apart in TiO_2 nanoparticles as dopants. Moreover, both **T1** and **T2** have a higher absorption in the whole range of 500–800 nm compared with that of the pure TiO_2 nanoparticles, which may indicate an increment of surface electric charge of TiO_2 [17]. In the case of **T2**, it is further found that a broad peak around 710 nm appears, which may be attributed to absorption of $CuInS_2$ [18]. These phenomena further indicate that the $CuInS_2$ clusters are incorporated in the TiO_2 nanoparticles. Meanwhile, there exist some electronic interactions between the TiO_2 nanoparticles and the $CuInS_2$ clusters, suggesting that the samples obtained probably exhibit a high photocatalytic activity.

The photocatalytic activities of the pure TiO_2 nanoparticles and **T1** for the degradation of 4-nitrophenol are shown in Fig. 4. From Fig. 4, it can be observed that the photolysis of 4-nitrophenol is slow (ca. 10% after 4 h irradiation) when the photocatalyst is absent. Compared with the pure TiO_2 nanoparticles, **T1** displays a higher photocatalytic activity with 99.9% of degradation ratio of 4-nitrophenol after 2 h irradiation. The introduction of the $CuInS_2$ clusters can obviously enhance the photocatalytic activity of the TiO_2 nanoparticles. The high photocatalytic activity of **T1** may be attributed to two causes. One is the inner electric field induced by the p–n junctions between the n-type TiO_2 and the p-type $CuInS_2$

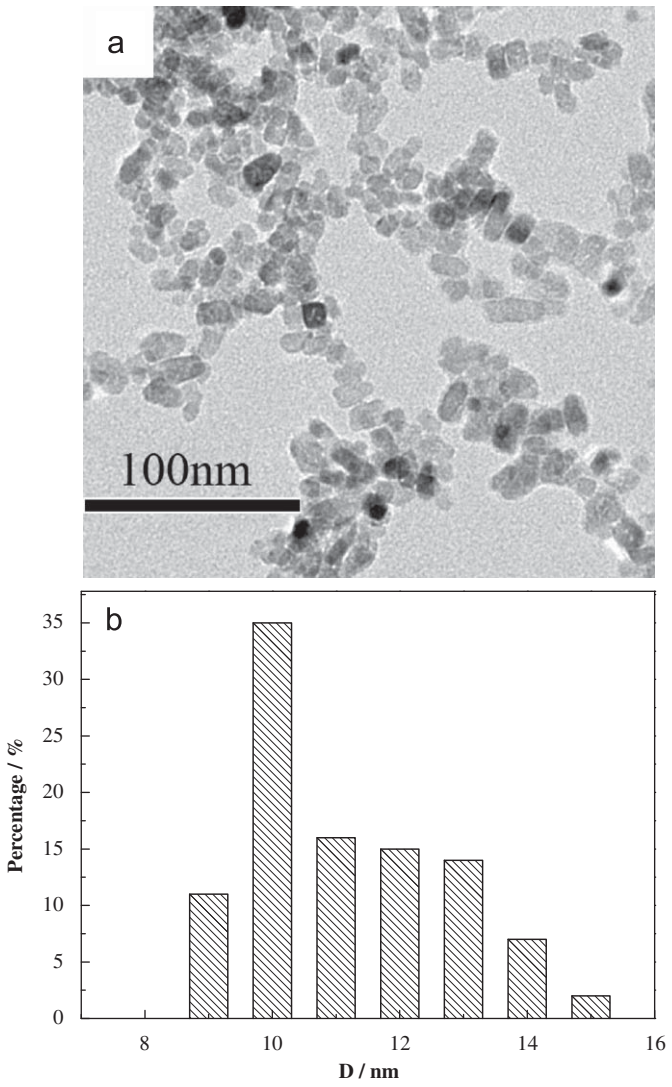

Fig. 2. TEM image of **T1** (a) and the size distribution histogram of particles (b).

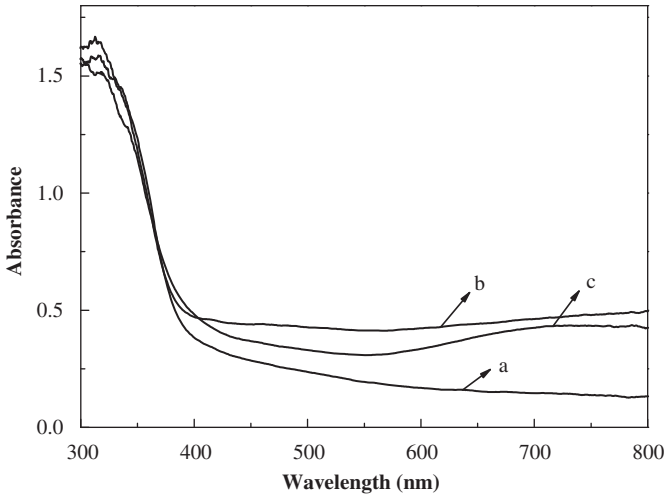

Fig. 3. Diffuse reflectance UV–Vis spectra of the pure TiO_2 nanoparticles (a), **T1** (b), and **T2** (c).

[19]. Another may be the interface between TiO_2 and $CuInS_2$, which can make effective charge separation. The results reported previously show that the conduction band edge (CB) of $CuInS_2$ is more negative than that of TiO_2. And the position of the valence band edge (VB) of $CuInS_2$ is close to that of the TiO_2 CB [20]. When **T1** is irradiated, the photogenerated holes stay in TiO_2 and electrons are just trapped at the interface between TiO_2 and $CuInS_2$, which will reduce the possibility of the electron–hole recombination.

The previous reports indicate that not only the oxidation but also the reduction of 4-nitrophenol can occur in the photocatalytic degradation. In a basic solution, the hydroxyl radical oxidation is the major reaction pathway [1,21]. Because the experiments are carried out at pH 4, it is suggested that the reduction of the nitro group in 4-nitrophenol is an important degradation pathway (Scheme 1). The $CuInS_2$ clusters may be the reactive sites of the reduction. The degradation process may be as follows: during the initial step, 4-nitrophenol is directly reduced by photogenerated electrons trapped at the interface between TiO_2 and $CuInS_2$ to produce 4-aminophenol. Then, 4-aminophenol is mineralized by •OH. Therefore, it can be deduced that, in comparison with the p–n junctions between the n-type TiO_2 and the p-type $CuInS_2$, the interface between TiO_2 and $CuInS_2$ may play a more important role in the enhancement of photocatalytic activity.

In order to further understand the role which the $CuInS_2$ clusters play in the photocatalyst, the PL spectra (Fig. 5) and photocurrent action spectra (Fig. 6) were measured at room temperature. As can be seen from Fig. 5, the photoluminescence of the TiO_2 nanoparticles incorporated with $CuInS_2$ clusters is apparently weaker than that of the pure TiO_2 nanoparticles, implying that the possibility of the electron–hole recombination

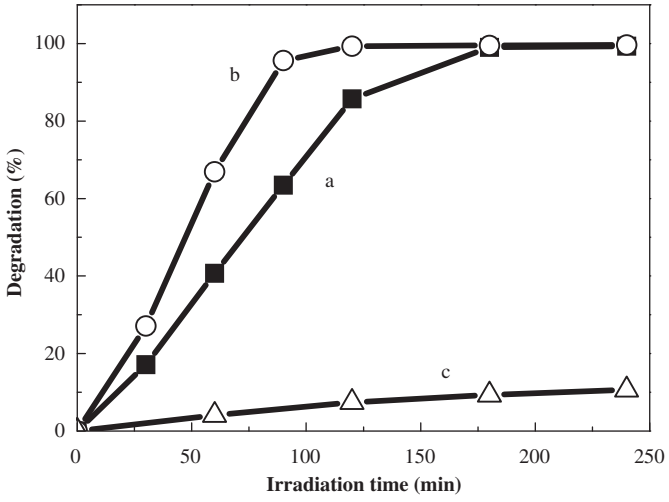

Fig. 4. Kinetic curves of 4-nitrophenol (1.44×10^{-4} mol L^{-1}) degradation under UV irradiation in the presence of the pure TiO_2 nanoparticles (a), **T1** (b), and in the absence of photocatalyst (c).

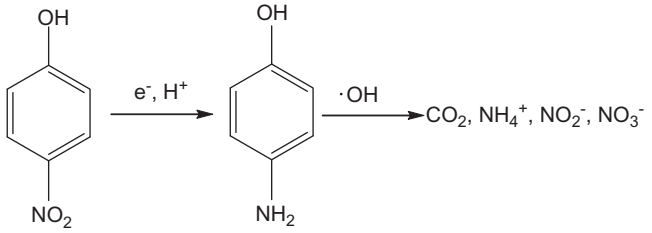

Scheme 1. Pathway proposed for the photocatalytic degradation of 4-nitrophenol.

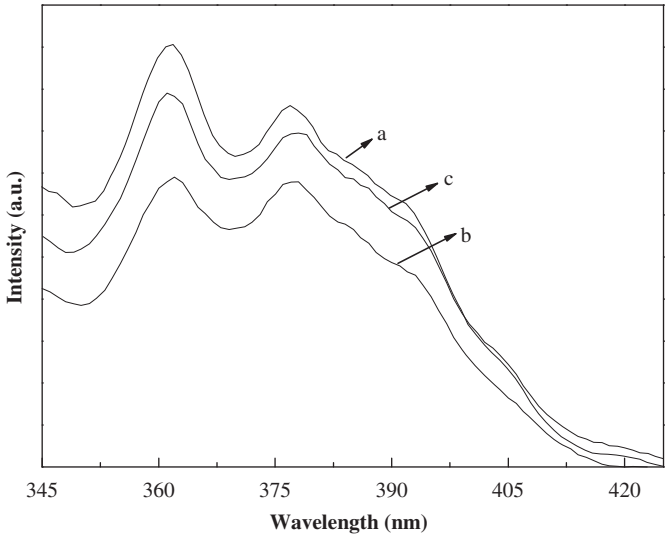

Fig. 5. Photoluminescence spectra of the pure TiO_2 nanoparticles (a), **T1** (b), and **T2** (c). The excitation wavelength is 325 nm.

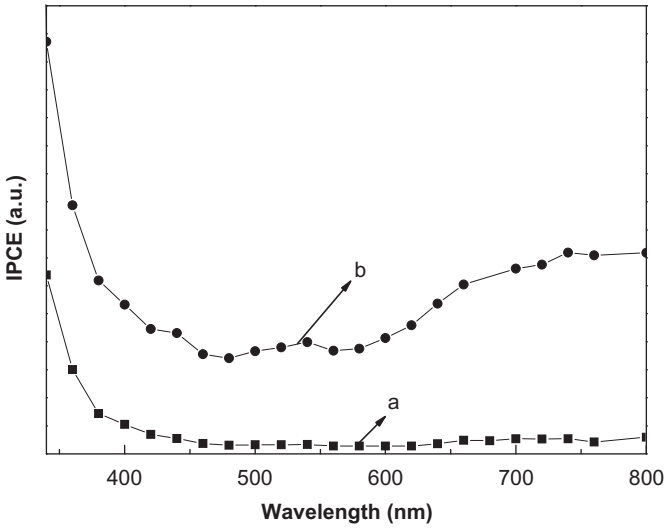

Fig. 6. Photocurrent action spectra of the pure TiO_2 nanoparticles (a) and **T2** (b).

is reduced due to introduction of the $CuInS_2$ clusters. Furthermore, the photocurrent action spectra of the pure TiO_2 nanoparticles and **T2** show that **T2** exhibits a high response in the range of 650–800 nm while the response of the pure TiO_2 nanoparticles is near zero. Combined with the results from UV–Vis spectra, it should be deduced that the response in the visible region arises from the absorption of the $CuInS_2$. Unfortunately, the photocatalytic degradation of 4-nitrophenol under the visible light irradiation ($\lambda > 420$ nm) is very low even in the presence of **T2**. One possible explanation is that the electrons move to the TiO_2 CB and the holes stay in the $CuInS_2$ VB under visible light irradiation. The above discussion indicates that the reduction is an important reaction pathway and the $CuInS_2$ clusters may be the reactive sites of the reduction. The accumulation of holes on the $CuInS_2$ clusters would be unfavorable to the reduction of 4-nitrophenol. Moreover, as was expected, it can be also seen from Fig. 6 that **T2** exhibits a higher incident photon-to-current conversion efficiency (IPCE) in the 340–800 nm region compared with the pure TiO_2 nanoparticles. In the case of UV light irradiation, since the holes are known to be trapped in TiO_2 and hard to move [22], the

Table 1
Dependence of the photocatalytic activity on the content of $CuInS_2$ after 90 min irradiation.

$CuInS_2$ contents (at%)	Degradation (%)
0	63.4
0.1	85
0.5	95.6
5	78.7

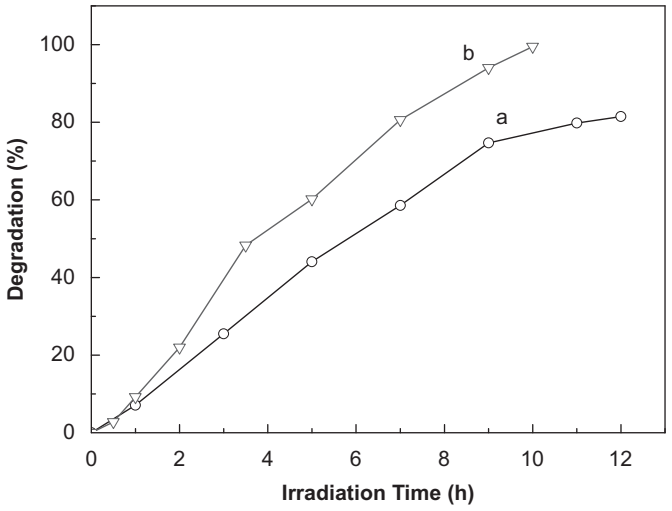

Fig. 7. Kinetic curves of 4-nitrophenol (1.44×10^{-4} mol L^{-1}) degradation under UV irradiation in the presence of the pure TiO_2 film (a) and the **T1** film (b).

improved separation of the photogenerated electrons and holes after the introduction of the $CuInS_2$ clusters may be ascribed to the interface between TiO_2 and $CuInS_2$. Therefore, the p–n junction effect should be neglected in comparison with the interface effect.

The dependence of the photocatalytic activity on the content of $CuInS_2$ is listed in Table 1. It can be noted that there is an optimal content of $CuInS_2$ (0.5 at%) for the photocatalytic decomposition of 4-nitrophenol. The photocatalytic activity of the TiO_2 nanoparticles incorporated with the $CuInS_2$ clusters increases from 0.1 to 0.5 at%. One possible explanation is that when the content of $CuInS_2$ is less than the optimal content, the $CuInS_2$ clusters would act as separation sites. On the contrary, when the content of $CuInS_2$ is more than the optimal content, the $CuInS_2$ clusters may become new recombination sites of the photogenerated electrons and holes [8]. In addition, in order to check potential use of the TiO_2 nanoparticles incorporated with the $CuInS_2$ clusters, **T1** was immobilized on the glass, and its photocatalytic behavior was also examined. Fig. 7 shows the relationship of the irradiation time and the degradation ratio of 4-nitrophenol. As can be seen from Fig. 7, 4-nitrophenol is nearly completely decomposed after 10 h irradiation when **T1** immobilized on the glass is used as the photocatalyst. Meanwhile, the introduction of the $CuInS_2$ clusters obviously enhances the photocatalytic activity of the TiO_2 nanoparticles. This result indicates that **T1** immobilized on the glass reserves a considerable photocatalytic activity, which is attractive for potential application.

4. Conclusions

In summary, the TiO_2 nanoparticles incorporated with the $CuInS_2$ clusters were prepared. The TiO_2 nanoparticles incorporated with the $CuInS_2$ clusters can display a very high photocatalytic activity with 99.9% of degradation ratio of 4-nitrophenol. The excellence photocatalytic activity should mainly be ascribed to the interface between TiO_2 and $CuInS_2$. Meanwhile, the photocatalyst immobilized on the glass still reserves a considerable photocatalytic activity, which is encouraging for the application in practical systems. The further efforts are currently being undertaken.

References

[1] A.D. Paola, V. Augugliaro, L. Palmisano, G. Pantaleo, E. Savinov, J. Photochem. Photobiol. A Chem. 155 (2003) 207–214.
[2] A. Alif, J.F. Pilichowski, P. Boule, J. Photochem. Photobiol. A Chem. 59 (1991) 209–219.
[3] Q.L. Wei, J. Mu, J. Dispersion Sci. Technol. 26 (2005) 555–558.
[4] C. Grasso, M. Nanu, A. Goossens, M. Burgelman, Thin Solid Films 480 (2005) 87–91.
[5] R. O'Hayre, M. Nanu, J. Schoonman, A. Goossens, Q. Wang, M. Gratzel, Adv. Funct. Mater. 16 (2006) 1566–1576.
[6] M.H. Priya, G. Madras, Ind. Eng. Chem. Res. 45 (2006) 482–486.
[7] T. Essam, M.A. Amin, O. El Tayeb, B. Mattiasson, B. Guieysse, Water Res. 41 (2007) 1697–1704.
[8] Y.L. Kuo, H.W. Chen, Y. Ku, Thin Solid Films 515 (2007) 3461–3468.
[9] F. Ye, A. Ohmori, C. Li, Surf. Coat. Technol. 184 (2004) 233–238.
[10] S. Gorai, S. Bhattacharya, E. Liarokapis, D. Lampakis, S. Chaudhuri, Mater. Lett. 59 (2005) 3535–3538.
[11] D. Chen, A.K. Ray, Appl. Catal. B Environ. 23 (1999) 143–157.
[12] G.P. Smestad, M. Gratzel, J. Chem. Educ. 75 (1998) 752–756.
[13] F. Song, L. Huang, D. Chen, W. Tang, Mater. Lett. 62 (2008) 543–547.
[14] F. Gracia, J.P. Holgado, A. Caballero, A.R. Gonzalez-Elipe, J. Phys. Chem. B 108 (2004) 17466–17476.
[15] S. Sakthivel, M.V. Shankar, M. Palanichamy, B. Arabindoo, D.W. Bahnemann, V. Murugesan, Water Res. 38 (2004) 3001–3008.
[16] P.K. Ghosh, R. Maity, K.K. Chattopadhyay, Sol. Energy Mater. Sol. Cells 81 (2004) 279–289.
[17] S.-Z. Kang, Z. Cui, J. Mu, Fullerenes Nanotubes Carbon Nanostruct. 15 (2007) 81–88.
[18] A.B. Mandale, S.D. Sathaye, K.R. Patil, Mater. Lett. 55 (2002) 30–33.
[19] Y. Chen, J.C. Crittenden, S. Hackney, L. Sutter, D.W. Hand, Environ. Sci. Technol. 39 (2005) 1201–1208.
[20] R. van de Krol, Y. Liang, J. Schoonman, J. Mater. Chem. 18 (2008) 2311–2320.
[21] V. Maurino, C. Minero, E. Pelizzetti, P. Piccinini, N. Serpone, H. Hidaka, J. Photochem. Photobiol. A Chem. 109 (1997) 171–176.
[22] Y. Tamaki, K. Hara, R. Katoh, M. Tachiya, A. Furube, J. Phys. Chem. C 113 (2009) 11741–11746.